Bioconjugate Chemistry

ARTICLE

pubs.acs.org/bc

Identification of Molecular-Mimicry-Based Ligands for Cholera Diagnostics using Magnetic Relaxation

Charalambos Kaittanis,[†] Tuhina Banerjee,[‡] Santimukul Santra,[†] Oscar J. Santiesteban,[§] Ken Teter,[‡] and J. Manuel Perez*[,†,‡,§]

[†]Nanoscience Technology Center, [‡]Burnett School of Biomedical Sciences — College of Medicine, [§]Department of Chemistry, University of Central Florida, 12424 Research Parkway, Suite 400, Orlando, Florida 32826, United States

Supporting Information

ABSTRACT: When covalently bound to an appropriate ligand, iron oxide nanoparticles can bind to a specific target of interest. This interaction can be detected through changes in the solution's spin−spin relaxation times (T2) via magnetic relaxation measurements. In this report, a strategy of molecular mimicry was used in order to identify targeting ligands that bind to the cholera toxin B subunit (CTB). The cellular CTB-receptor, ganglioside GM1, contains a pentasaccharide moiety consisting in part of galactose and glucose units. We therefore predicted that CTB would recognize carbohydrate-conjugated iron oxide nanoparticles as GM1 mimics, thus producing a detectable change in the T2 relaxation times. Magnetic relaxation experiments demonstrated that CTB interacted with the galactose-conjugated nanoparticles. This interaction was confirmed via surface plasmon resonance studies using either the free or nanoparticle-conjugated galactose molecule. The galactose-conjugated nanoparticles were then used as CTB sensors achieving a detection limit of 40 pM. Via magnetic relaxation studies, we found that CTB also interacted with dextran-coated nanoparticles, and surface plasmon resonance studies also confirmed this interaction. Additional experiments demonstrated that the dextran-coated nanoparticle can also be used as CTB sensors and that dextran can prevent the internalization of CTB into GM1-expressing cells. Our work indicates that magnetic nanoparticle conjugates and magnetic relaxation detection can be used as a simple and fast method to identify targeting ligands via molecular mimicry. Furthermore, our results show that the dextran-coated nanoparticles represent a low-cost approach for CTB detection.

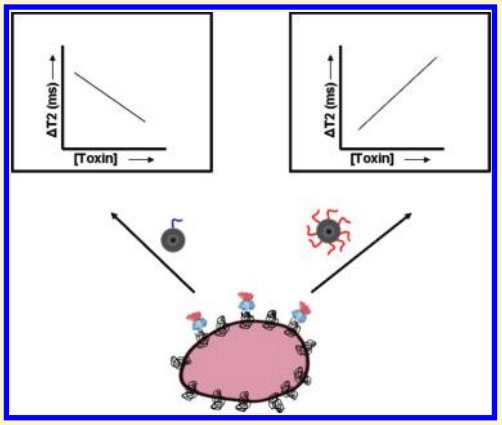

INTRODUCTION

Many bacteria and fungi produce toxins that can effectively cause disease.[1,2] *Bacillus anthracis* produces the potent anthrax toxins, *Clostridium botulinum* produces the botulinum neurotoxins, enterohemorrhagic *Escherichia coli* and *Shigella dysenteriae* make the Shiga toxins, and *Clostridium perfringens* produces the epsilon toxin, whereas *Vibrio cholerae* secretes the cholera toxin (CT). Apart from causing substantial pathogenesis after environmental exposure, these toxins can be used in bioterrorism. Therefore, developing sensitive and robust diagnostic modalities for these agents is of major importance. However, current toxin detection methods primarily rely on antibody−antigen interactions, rendering these assays laborious and expensive.[3] Likewise, common therapeutic approaches typically involve either the administration of neutralizing antibodies, such as those against the tetanus toxin, to sequester and eliminate the toxin from circulation[4] or the rapid oral and intravenous administration of fluids, like in the case of cholera toxins.[5] An attractive alternative route for toxin diagnostics and treatment is to rationally design molecular entities that firmly interact with their target to (i) quickly yield a high detection signal even at low toxin concentrations or (ii) interact with the toxin to inhibit its pathogenesis and capability to infect cells.

Since early detection is critical for the prevention of intoxication outbreaks, toxins have to be identified quickly and reliably. Current toxin detection methods utilize antibody−antigen interactions via ELISA,[6] Western blots,[7,8] antibody microarrays,[9] surface plasmon resonance (SPR) biosensors,[10] and antibody-coated polystyrene microbeads.[11] These methods are relatively sensitive and have multiplexing capabilities but typically require toxin purification procedures that are critical for assay sensitivity and specificity, as they minimize background noise. Thus, limited biological and environmental samples can be screened. Liquid chromatography mass spectrometry[12] and multidimensional protein identification[13] can achieve highly sensitive toxin detection. However, these techniques use sophisticated instrumentation that lacks portability and is difficult to operate, which

Received: October 6, 2010
Revised: December 2, 2010
Published: January 12, 2011

prevents the broader use of these diagnostic methods. Similarly, cell-based systems, that beyond assessing interaction can determine the toxin's activity, tend to be time-consuming.[14] Hence, identifying novel toxin targeting ligands that can be used to develop cheap, fast, and deployable diagnostics or treatment regimes is highly important.

One way to identify small-molecule ligands that can selectively bind to a toxin is to inspect the molecular interactions that occur between the toxin and the amino acids or carbohydrate groups on the protein receptor that bind to the toxin. This type of molecular-mimicking investigation could result in the identification of amino acids or carbohydrate-based targeting ligands that selectively bind to the toxin of interest. This information can therefore be used to design sensitive toxin diagnostics and therapeutic agents. A powerful tool for the determination of these molecular interactions is surface plasmon resonance (SPR) analysis. SPR is a label-free technique that allows the identification of specific associations between biomolecules attached to a gold surface and their targets in buffered solutions. The binding event is assessed optically by measuring the interaction of incident light photons with free electrons on the gold surface (surface plasmons) in the presence or absence of the binding molecule. However, due to its optical nature, SPR requires a homogeneous nonturbid solution that can be a problem with some environmental and biological samples.

An optically independent strategy is to use magnetic methods utilizing iron-oxide-based magnetic nanoparticles. In this case, the classical label is replaced by a superparamagnetic nanoparticle, which can be detected magnetically using the intrinsic magnetic properties of the nanoparticle's core. Examples include superconductive-quantum-interference-device-based (SQUID) detection, hand-held magnetic readers, giant magneto-resistive detectors, and MagArray Chips.[3,15] Similar to SPR, these techniques rely on the binding of the substrate to a solid surface. Another alternative magnetic method performed in solution employs magnetic relaxation nanoswitches (MRnS), which are composed of superparamagnetic iron oxide nanoparticles conjugated with targeting ligands that exhibit changes in the solution's spin−spin relaxation times ($\Delta T2$) upon target binding.[16,17]

MRnS techniques have been primarily developed for the detection of biomolecular targets, including DNA, proteins, enzymatic activity, viruses, bacteria, and cancer cells.[16−22] In all of these cases, a ligand (DNA, antibody, or small molecule) known to interact with the corresponding biological target has been immobilized on the superparamagnetic nanoparticles to facilitate association and magnetic relaxation detection. We hypothesized that MRnS, similar to SPR, can be used to screen an unknown ligand−biomolecule interaction with the goal of developing sensitive diagnostics and therapeutics. In contrast to SPR and other magnetic methods, MRnS is a homogeneous assay that does not involve binding of a biomolecule to a surface and can be done using opaque or colored media. An additional benefit of MRnS is that a multivalent ligand display on the nanoparticle surface can be achieved. This accomplishes the study of multivalent target interactions by engineering low-valency (LV) and high-valency (HV) nanoparticles. In addition, since the targeting ligands are already bound to the magnetic nanoparticle label, assessing their interaction with the target in solution would be a better predictor of how these interactions will occur when the magnetic nanoparticle conjugates are used in diagnostic assays and therapeutic regimes.

Scheme 1. Structure of the GM1 Ganglioside Found on Intestinal Epithelial Cells and Binding of Cholera Toxin (CT) to the Target Cells[a]

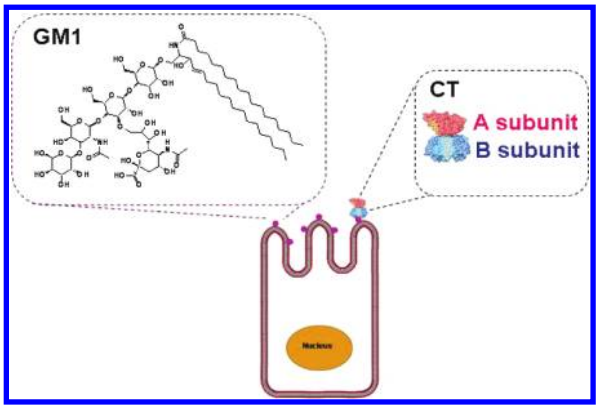

[a] GM1 gangliosides, located on the surface of the target cells, are the known ligands that facilitate binding and internalization of CT. *N*-Acetylgalactosamine (GalNAc), *N*-acetylneuraminic acid (Neu5Ac), glucose (Glc), and galactose (Gal) residues comprise the pentasaccharide moiety of the GM1 ganglioside facilitating interaction with the B subunit of cholera toxin (CTB).

Since MRnS have not been previously utilized for the identification and validation of a previously unknown molecular interaction, herein we used molecular mimicry to screen the interaction of carbohydrates present in the known target (GM1 gangliosides) of the CT. CT is produced by the bacterium *Vibrio chlolerae*, which is one of the most common water-borne pathogens causing gastrointestinal disorders.[5] CT belongs to the class of AB-type protein toxins that consist of a monomeric catalytic A subunit and a cell-binding homopentameric B subunit.[23] Binding of the B subunit (CTB) to GM1 gangliosides at the cell surface of intestinal epithelial cells causes the toxin to be endocytosed and delivered to the endoplasmic reticulum, through a series of vesicular trafficking events.[5] The catalytic A1 subunit then dissociates from the toxin and crosses the membrane of the endoplasmic reticulum to reach the cytosol where its target—Gsα—is located.[24] Toxin activity against Gsα generates an intracellular signaling cascade that eventually leads to the opening of chloride channels on the apical face of affected intestinal epithelial cells. Water follows chloride efflux into the gut, leading to the profuse and potentially fatal diarrheic response to infection with *V. cholerae*.[5] Since CTB binds GM1 ganglioside via interactions with its pentasaccharide moiety containing *N*-acetylgalactosamine (GalNAc), *N*-acetylneuraminic acid (Neu5Ac), glucose (Glc), and galactose (Gal) residues (Scheme 1),[23,25] we hypothesized that CTB would bind to magnetic nanoparticles coated with carbohydrate constituents of GM1. We anticipated that this interaction would generate changes in T2 that could be used for screening these interactions with the goal of identifying small molecule ligands useful for the development of sensors and potentially therapeutic agents for cholera. Using this approach, we confirmed by both SPR and MRnS that galactose binds to CTB. Furthermore, we showed that an MRnS−galactose conjugate can detect CTB via magnetic relaxation with a detection limit of 40 pM. We further discovered via magnetic relaxation and later confirmed by SPR that dextran—a glucose polymer—can bind to CTB. For the magnetic relaxation assessment, a dextran-coated iron oxide nanoparticle was simply used as the MRnS

probe, which was capable of achieving a CTB detection threshold of 16 nM. Further SPR analysis confirmed the interaction of CTB with dextran with a calculated dissociation constant (K_D) of 14 mM. As suggested, using MRnS we studied the effect of a multivalent ligand display and found that the valency of the MRnS affected the $\Delta T2$ pattern, but not the sensitivity of the system. Additionally, since binding between CTB and dextran has not been previously reported, we confirmed this interaction with a cell-based competition assay in which increasing concentrations of dextran led to the inhibition of CTB binding at the cell surface. This hints the potential use of dextran-based therapeutics in the treatment of cholera. Taken together, our work suggests that magnetic relaxation can be used in the assessment and development of molecular-mimicking systems for potential MRnS-based diagnostics applications. Using molecular-mimicry-based MRnS and cholera toxin as a model system, we have discovered that dextran-coated nanoparticles can be used for the fast, cheap, homogeneous, and single-step detection of cholera toxin.

EXPERIMENTAL PROCEDURES

Reagents. All reagents were of analytical reagent grade. Iron salts ($FeCl_2 \cdot 4H_2O$ and $FeCl_3 \cdot 6H_2O$) were obtained from Fluka. Polyacrylic acid (PAA, MW 1.8 kDa), ammonium hydroxide, hydrochloric acid, *N*-hydroxysuccinimide (NHS), and the CTB pentamer were purchased from Sigma-Aldrich, whereas Dextran (MW 10 kDa) was received from Pharmacosmos. EDC (1-ethyl-3-[3-dimethylaminopropyl]carbodiimide hydrochloride), SPDP (*N*-succinimidyl 3-(2-pyridyldithio)-propionate), and DTT (dithiothreitol) were obtained from Pierce Biotechnology, and the Tetanus toxin C fragment (TTC) was from Roche Biomedical.

Synthesis of Dextran-Coated MRnS and Galactose-Carrying High-Valency and Low-Valency MRnS. Dextran-coated MRnS were prepared as previously reported.[20] Aminated PAA-coated nanoparticles were synthesized in accordance to the literature,[26] and conjugation of galactopyranosyl nonanoic acid (Toronto Research Chemicals; MW 336.38) was achieved via carbodiimide chemistry, yielding either high-valency (HV MRnS) or low-valency nanosensors (LV MRnS). Specifically for the LV MRnS, 200 μL of aminated polyacrylic-acid-coated iron oxide nanoparticles (PAA NP) ([Fe] = 2.5 μg/μL) were reacted with the carboxylated galactose (6 mg in 1000 μL DI water/DMSO 50:50 v/v) in the presence of EDC and NHS (9.5 and 5.5 mg, respectively, in 1000 μL MES buffer). In the case of HV MRnS, 214 μL of PAA NP were reacted with 15 mg of the carboxylated galactose (15 mg in 150 μL DMSO plus 36 μL 0.1 M $NaHCO_3$ buffer), in the presence of EDC−NHS (14 and 5 mg, respectively, in 250 μL MES buffer). The reactions were carried out overnight at 4 °C under constant mixing, followed by dialysis (6000−8000 MWCO) and magnetic separation.

Determination of the Number of Conjugated Galactose Molecules. In order to assess the average number of galactose molecules per nanoparticle, we followed a previously published methodology, based on the quantification of amino groups per nanoparticle.[27,28] Specifically, we first determined the number of amino groups on the PAA NP ([Fe] = 2.5 mg/mL) and HV/LV MRnS ([Fe] = 1.5 mg/mL). Initially, 200 μL aliquots of each preparation were mixed with 100 μL SPDP (75 mM) and 100 μL sodium phosphate buffer (0.1 M, pH 7.4). After a 2 h incubation at room temperature under continuous mixing, the solutions were filtered using a PD10 column (GE Healthcare Life Sciences), facilitating the isolation of SPDP-activated nanoparticles. Fifty microliters of the isolated nanoparticles were added to 300 μL sodium phosphate buffer (0.1 M, pH 7.4) and 75 μL DTT (20 μm), followed by a 2-h-long incubation at room temperature. Subsequently, the released pyridine-2-thione was isolated through centrifugation at 10 000 rpm using a Centricon filter unit (MWCO: 30 000, Millipore), and its absorbance was recorded at 343 nm using a Genesys 20 spectrophotometer (Thermo Scientific). Finally, this allowed the determination of the number of free amino groups and galactose molecules on LV MRnS (on average, 11 NH_2 groups and 34 Gal molecules) and HV MRnS (on average, 45 Gal molecules), as the precursor PAA NP had 45 amino groups on average.

Magnetic-Relaxation-Mediated Detection of CTB. Serial dilutions of CTB were prepared in DI water. Five microliter aliquots of CTB were incubated with 195 μL of MRnS working solutions ([Fe] = 0.001 μg/μL) at room temperature. Spin−spin relaxation times (T2) were recorded via the 0.47T mq20 NMR analyzer (Minispec, Bruker).

SPR Studies for the Toxin-Sensing MRnS. GM1-coated slides were prepared as previously described,[29] by applying 50 μL of the ganglioside (3 ng/μL, Sigma) directly to the surface of a Reichert gold plate sensor. The plate was allowed to air-dry for 30 min at room temperature. Afterward, CTB was bound to the GM1-coated sensor by perfusing 10 μg/mL of the CTB pentamer over the slide for 10 min at a flow rate of 5 μL/min. CTB was diluted in phosphate buffered saline containing 0.05% Tween-20 (PBST) at pH 7.4. The same methodology was followed in order to prepare slides with TTC, through the prior deposition of the GD1b ganglioside (Sigma) on the surface of the sensor slide. SPR experiments were performed on a Reichert SR7000 SPR refractometer. Before adding the experimental samples, PBST (pH 7.4) was perfused over the sensor slide for 5 min, in order to establish a baseline reading. The samples, diluted in PBST, were then flowed over the sensor slide. Ligand binding to the toxin-coated sensor slide led to an increase in the mass on the slide. This shift in mass generated a change in the resonance angle of the reflected light, which was recorded as a change in the refractive index unit (MicroRU). After each reading, any remaining bound ligand was removed from the sensor slide with a 5 min PBST wash at pH 6.0. The flow rate for all steps was 5 μL/min. The Reichert *Labview* software was used for data collection.

SPR-Based Determination of the Dextran−CTB Interaction. An EDC-NHS activation buffer was perfused over a Reichert gold-plated glass slide for 10 min at a flow rate of 5 μL/min. The same flow rate was used for all subsequent steps. A 5 min wash with PBST at pH 7.4 was used to remove the activation buffer, after which an anti-CTB antibody (Calbiochem) at 1:2000 dilution in sodium acetate (pH 5.5) was perfused over the slide for 15 min. Any unbound antibody was removed with a 5 min PBST wash, and the remaining active groups on the sensor slide were deactivated with a 3 min exposure to ethanolamine. After a 5 min wash with PBST, the CTB pentamer was perfused over the slide for 10 min at a concentration of 100 μg/mL. PBST was flowed over the CTB-coated slide for another 10 min to establish a stable baseline signal. Solutions of different dextran concentrations (0.25, 0.50, 0.75, 1.0, and 1.50 mg/mL) in PBST were then perfused over the sensor slide. Samples were removed from the perfusion buffer after approximately 400 s. After each reading, any remaining bound ligand was removed from the sensor slide with a 5 min PBST wash at pH 6.0. The Reichert

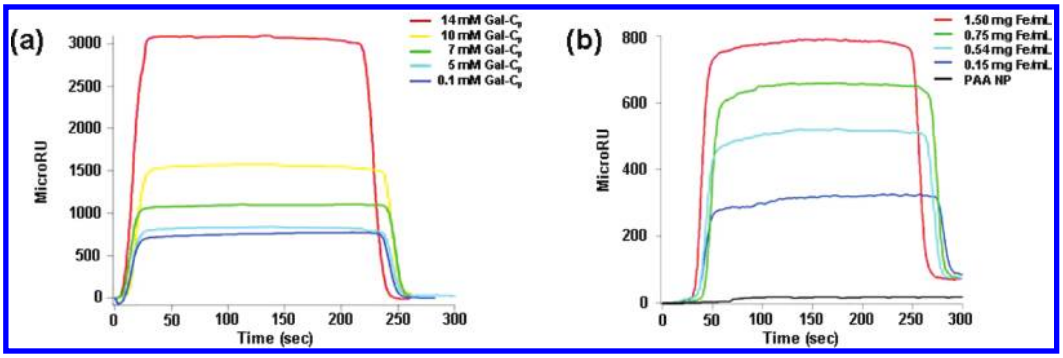

Figure 1. Detection of the CTB−galactose interaction by SPR. (a) Unconjugated galactose (galactopyranosyl nonanoic acid; Gal-C_9) was perfused at the stated concentrations over an SPR sensor slide coated with the CTB pentamer. Ligand was removed from the perfusion buffer 150 s into the experiment. (b) Galactose-carrying MRnS were perfused at the stated iron concentrations over an SPR sensor slide coated with the CTB pentamer. PAA NP were also perfused over the slide at a concentration of 1.5 mg/mL. The nanoparticles were removed from the perfusion buffer 150 s into the experiment.

Labview software was used for data collection. Interaction curves obtained for dextran were analyzed with a Langmuir 1:1 binding kinetic analysis using the BioLogic (Campbell) *Scrubber 2* software.

Binding of CTB to the Plasma Membrane in the Presence of Dextran. Vero cells were seeded on 96-well clear-bottom black-walled plates (Greiner Bio-One), in order to be at 75% confluency after 2 days of incubation at 37 °C. Twelve wells were seeded for each condition. When the cells reached the desired confluency (75%), they were washed once with PBS and incubated at 4 °C with serum-free Ham's F-12 culture medium containing 1 μg/mL of a CTB pentamer conjugated with fluorescein isothiocyanate (FITC-CTB; Sigma). The medium also contained various concentrations of dextran to yield dextran/FITC-CTB molar ratios of 0.5:1, 1:1, 2:1, 4:1, 10:1, 50:1, and 100:1. After 30 min at 4 °C, the cells were washed once with PBS and then placed in PBS for fluorescence measurement using a Biotek Synergy 2 plate reader. Fluorescence was read at an excitation of 485/20 nm and an emission of 528/20 nm. Measurements obtained from Vero cells incubated in the absence of FITC-CTB were set as the background and subtracted from all other results. Data were expressed as percentages of the maximum fluorescent signal from cells incubated with FITC-CTB in the absence of dextran.

RESULTS

Interaction of Galactose and Galactose-Carrying MRnS with CTB. Galactose is a component of the GM1 ganglioside,[23,25] so we hypothesized that a galactose-carrying MRnS would resemble GM1 and therefore bind to the pentameric CTB. A previous study using fluorescence spectroscopy has indeed shown that pure galactose interacts with the CTB pentamer.[30] To test our hypothesis, we first determined by SPR whether pure galactose and galactose-carrying MRnS binds to CTB. We synthesized the galactose-carrying MRnS via conjugation of carboxylic-acid-terminated galactose (galactopyranosyl nonanoic acid) to aminated polyacrylic-acid-coated iron oxide nanoparticles (d = 75 nm, $r2$ = 210 M^{-1} s^{-1}). As shown in Figure 1a, pure galactose bound to the CTB-coated SPR sensor slide in a dose-dependent manner (Figure 1a). Galactose-carrying MRnS also bound to the CTB-coated sensor slide (Figure 1b), indicating that galactose conjugation to the iron oxide nanoparticle did not block the interaction between galactose and CTB. As expected, the aminated polyacrylic-acid-coated nanoparticles (PAA NP) did not interact with the CTB subunit, demonstrating the specificity of interaction between CTB and galactose-carrying MRnS. Likewise, neither galactose (i.e., galactopyranosyl nonanoic acid) nor galactose-carrying MRnS produced a MicroRU signal when they were perfused over a TTC-coated SPR sensor slide (Supporting Information Figure 1). The specificity of the galactose−MRnS toward CTB and not TTC could be due to the fact that TTC recognizes the gangliosides GD1b and GT1b in an event that appears to primarily involve the gangliosides' terminal sialic acid residues, rather than other carbohydrate components that can be found in GM1.[31,32] Therefore, galactose-carrying MRnS act as a specific molecular mimic for GM1, distinguishing between CTB and TTC.

To assess the utility of MRnS in toxin detection and to examine the effect that a multivalent presentation of galactose ligands would have on the detection threshold, we prepared galactose-carrying MRnS with low valency (LV) and high valency (HV). LV-galactose-MRnS and HV-galactose-MRnS were independently obtained by altering the stoichiometry of the conjugation reaction, as described in the Experimental Procedures section. Through spectrophotometric studies based on the release of pyridine-2-thione from activated nanoparticles, we found that the PAA NP contained 45 amino groups on the particle surface. LV MRnS had only 11 free amino groups remaining on the particle surface. Hence, 34 of the amino groups on the LV MRnS carried galactose conjugates. HV MRnS had no free amino groups on their surface, indicating that all 45 amino groups had reacted with the carboxylated galactose. Thus, the valency of HV MRnS was increased by ~33% in comparison to LV MRnS.

Consistent with previous findings on LV-folate-MRnS for cell detection,[19] magnetic relaxation studies with LV-galactose-MRnS recorded a linear concentration-dependent trend (Figure 2a). LV-galactose-MRnS exhibited a high $\Delta T2$ at low CTB concentrations and a low $\Delta T2$ at high CTB concentrations. With increasing CTB concentrations, the $\Delta T2$ signal approached the baseline background measurement ($\Delta T2 \leq$ 1.5 ms, SE = ± 0.1 ms) obtained with the TTC fragment. Magnetic relaxation experiments with LV-galactose-MRnS can easily distinguish between CTB and TTC within 5 min and can be used to quickly screen for targeting ligands that bind one toxin versus the other. Furthermore, LV-galactose-MRnS exhibited a very sensitive CTB detection threshold of 40 pM. Hence, it is anticipated that, as the LV MRnS can detect as little as 40 pM of CTB (0.2 ng/100 μL), similar MRnS can be used for the detection of powerful neurotoxins, like the botulinum toxin that has a lethal dosage of 90 ng.[33]

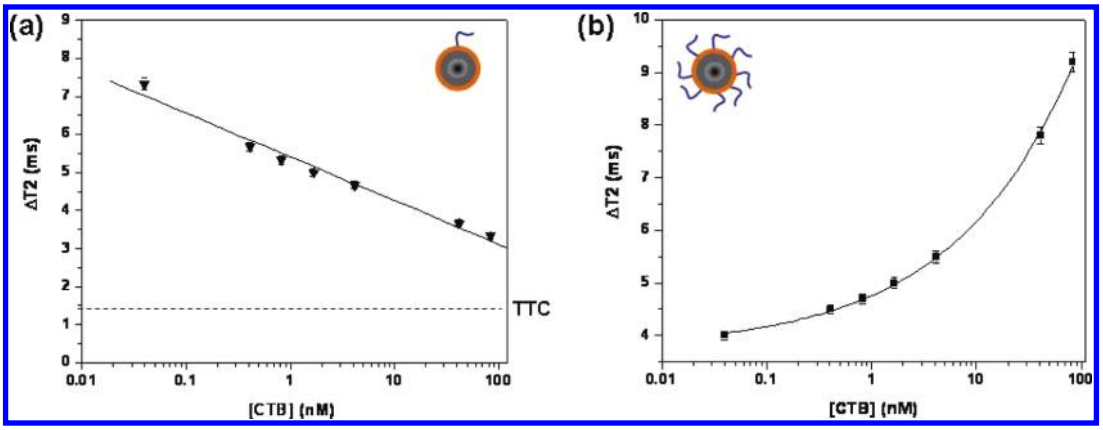

Figure 2. Specific detection of CTB with galactose-conjugated MRnS. Measurements involving the indicated concentrations of CTB were taken after a 5 min incubation with (a) LV or (b) HV galactose-conjugated MRnS. The means ±SE of three independent experiments are shown. The background signal obtained from 38 nM of TTC is presented in panel (a).

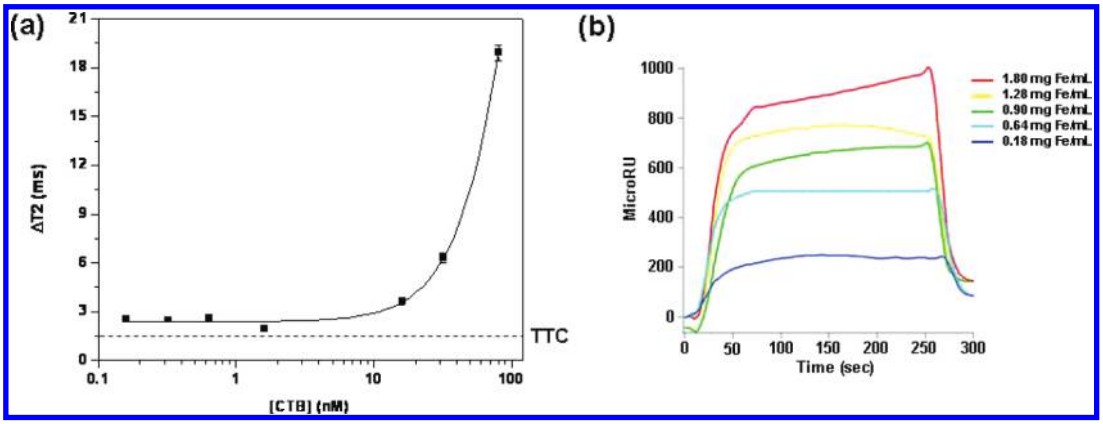

Figure 3. MRnS-based identification of dextran as a specific CTB ligand. (a) Magnetic relaxation measurements involving the indicated concentrations of CTB were taken after 5 min incubation with dextran-conjugated MRnS. The means ± SE of three independent experiments are shown. The background signal obtained from 38 nM of TTC is shown as a dotted line. (b) Dextran−MRnS were perfused at the stated concentrations over an SPR sensor slide coated with the CTB pentamer. The nanoparticles were removed from the perfusion buffer 130 s into the experiment.

In contrast, magnetic relaxation studies with the HV-galactose-MRnS revealed a dose-dependent trend that was different from the pattern observed with LV-galactose-MRnS. Specifically, increasing concentrations of CTB increased the $\Delta T2$ for the HV MRnS. The observed increase in $\Delta T2$ for HV-galactose-MRnS with increasing concentrations of galactose (Figure 2b) and a decrease $\Delta T2$ for LV-galactose-MRnS (Figure 2a) was in accordance with a previous report on the role of ligand valency on cancer cell detection using MRnS.[19] Despite the distinct $\Delta T2$ trends, both HV-galactose-MRnS and LV-galactose-MRnS could detect as little as 40 pM of CTB. The absence of any changes in $\Delta T2$ when TTC was incubated with HV-galactose-MRnS ($\Delta T2 \leq 1.5$ ms, SE = ±0.2 ms) further indicated that these galactose-carrying nanosensors specifically recognized CTB. The presentation of a higher number of galactose ligands on the magnetic nanoparticle does not affect the specificity of the galactose−MRnS toward CTB or increase the binding toward TTC. As in LV-galactose-MRnS, HV-galactose-MRnS can also distinguish between CTB and TTC within 5 min of incubation. Overall, these results indicate that MRnS can be used as a faster yet equally sensitive and selective alternative method to SPR for the identification of novel ligands and compounds that can serve as toxin sensors.

Identification of Dextran as a CTB Ligand Using MRnS. To design the galactose MRnS, we selected PAA NP over the most commonly used dextran-coated nanoparticles, since dextran being a glucose polymer could have also affected the binding with CTB. Like galactose, glucose is a component of the GM1 pentasaccharide.[23,25] Therefore, we hypothesized that dextran could represent another possible molecular mimic for CTB detection. As its monomeric building block is glucose, we reasoned that dextran could specifically bind to CTB and not to TTC. Consequently, in order to quickly assess by magnetic relaxation the binding of dextran to CTB, we utilized dextran-coated iron oxide nanoparticles as a dextran−MRnS system for the detection of CTB. These polymer-coated nanoparticles had a diameter of 115 nm and an $r2$ relaxivity of 175 mM^{-1} s^{-1}. After a 5 min incubation at room temperature, magnetic relaxation experiments in water revealed a concentration-dependent trend with a CTB detection limit of 16 nM (Figure 3a). Interestingly, the dextran-MRnS behaved as a high valency MRnS for the detection of CTB, as high CTB concentrations generated a high $\Delta T2$ signal. Nominal changes in the $\Delta T2$ ($\Delta T2 \leq 1.5$ ms, SE = ±0.2 ms) were recorded in the presence of TTC, demonstrating the specificity of CTB detection with the dextran−MRnS. SPR experiments confirmed that the dextran-coated

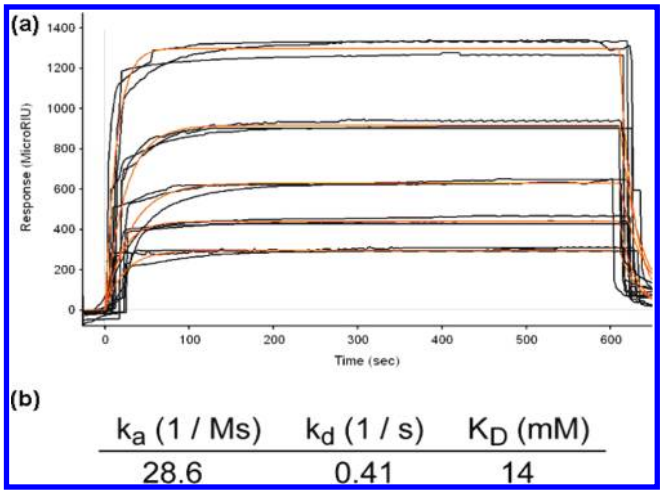

Figure 4. Affinity of dextran for CTB. (a) Dextran concentrations of 0.25, 0.50, 0.75, 1.0, and 1.5 mg/mL were perfused over an SPR sensor slide coated with the CTB pentamer. Measurements from three independent experiments with each dextran concentration are shown. The orange lines represent best fit curves derived from the raw data. (b) The aggregate data from panel (a) were used to calculate the on rate (k_a), off rate (k_d), and equilibrium dissociation constant (K_D) for the interaction between dextran and CTB.

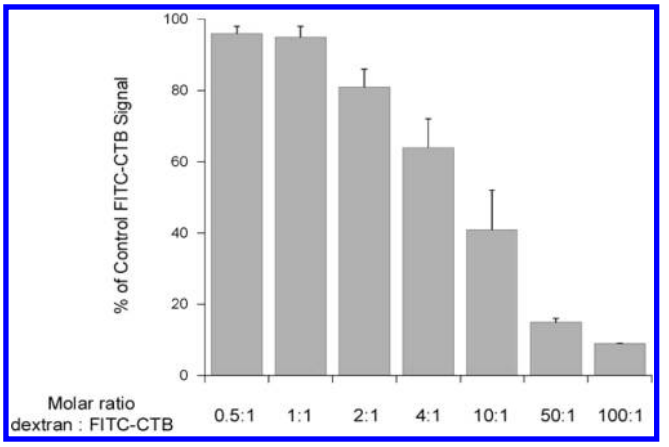

Figure 5. Dextran inhibits the binding of CTB to the cell surface. Vero cells were placed on ice and incubated with FITC-CTB for 30 min in the absence or presence of various dextran concentrations. The cells were washed with PBS to remove unbound toxin, and fluorescent output was determined with a plate reader. The signal obtained from control cells incubated with FITC-CTB in the absence of dextran was set at 100%, and all other results were expressed as percentages of that value. For dextran/FITC-CTB molar ratios of 50:1 and 100:1, results represent the averages ± ranges of two independent experiments. For all other conditions, results represent the averages ± standard errors of the means of 3−5 independent experiments.

MRnS bound to the CTB-coated sensor slide (Figure 3b), but not to the TTC-coated sensor slide (Supporting Information Figure 1). These results confirmed that MRnS along with magnetic relaxation detection can quickly (within minutes) identify molecular interactions that can later be confirmed by SPR. However, SPR cannot distinguish between low and high valency interactions, as shown here for the interaction of CTB with dextran-MRnS.

Interaction of Dextran with CTB. Considering that dextran was identified as an affinity ligand for CTB through the use of dextran-coated nanoparticles and magnetic relaxation, we employed SPR to establish the binding affinity between CTB and dextran. For these experiments, we used pure dextran and not dextran−MRnS. As shown in Figure 4a, dextran exhibited a dose-dependent interaction with the CTB pentamer (Figure 4a). The experiment was performed three times, and the aggregate data were used to calculate an equilibrium dissociation constant (K_D) of 14 mM for dextran and CTB (Figure 4b). Interestingly, this value was similar to the CTB K_D values of 40 mM for galactose and 81 mM for lactose, as calculated by fluorescence spectroscopy.[30] Dextran did not produce an SPR signal when perfused at a concentration of 14 mM over a TTC-coated SPR sensor slide (Supporting Information Figure 1), confirming our MRnS results. This demonstrated the specificity of the dextran−CTB interaction and further suggested that the glucose component of GM1 actively participates in the CTB binding event during cholera intoxication.

Finally, since dextran has never been shown to bind CTB, we utilized a cell-based assay to confirm the interaction between dextran and CTB. In these experiments, Vero cells expressing GM1 on their surface were incubated with dextran and fluorescein-labeled CTB (FITC-CTB) at 4 °C, a temperature that allows toxin binding to the cell surface but prevents endocytosis of the bound toxin. After a 30 min incubation, unbound toxin was removed and the fluorescent signal from bound FITC-CTB was recorded with a plate reader. As shown in Figure 5, dextran prevented FITC-CTB binding to the cell surface in a dose-dependent manner (Figure 5). An inhibitory effect was only observed with relatively high molar ratios of dextran/FITC-CTB, which was consistent with the differential interactions between CTB and dextran (low mM affinity) vs CTB and GM1 (low nM affinity[31,32]). Hence, using molecular mimicry and MRnS, herein we have identified a potential candidate (dextran) that interacts with CTB and can be utilized in the design of sensitive nanotechnology-based cholera diagnosis systems and potentially in effective cholera therapeutics. Also, for the first time, confirmation of the MRnS discovery and further characterization of the dextran−CTB interaction was established through SPR and cell-based assays.

DISCUSSION

The use of magnetic relaxation switches (MRnS) is an emerging technology that has been utilized for the sensitive and fast detection of clinically relevant biomolecules, cells, and metabolic activity in complex media.[16−21,34] The labels for this technique usually consist of a superparamagnetic iron oxide core with a stabilizing polymer coating that facilitates bioconjugation of targeting molecules. For instance, MRnS have been conjugated with antibodies to detect low populations of bacteria[18] and with folate to detect cancer cells that overexpress the folate receptor.[19] Hence, the common motif of these MRnS was the conjugation of known targeting moieties to the iron oxide nanoparticles, conferring specificity and sensitivity to the resulting probes. However, in the present study we have used molecular mimicry to identify by magnetic relaxation and confirm by SPR that galactose and dextran interact with CTB. This information has been used to develop selective magnetic relaxation nanoswitches to detect CT.

Binding of CTB to its cellular target occurs via interactions with GM1 pentasaccharide moieties on the cell surface, which contain *N*-acetylgalactosamine, *N*-acetylneuraminic acid,

glucose, and galactose residues.[23,25] We hypothesized that a GM1 molecular mimicking surface could be recreated by attaching some of these carbohydrates on the surface of magnetic nanoparticles, facilitating CTB binding and detection by changes in magnetic relaxation (T2 relaxation times). Previous work has shown that galactose, fucose, and lactose bind to CTB.[30] In addition, lactose-conjugated gold nanoparticles have also been used in a colorimetric assay for CTB detection.[35] In this work, we provide the first report of dextran as a CTB-binding carbohydrate and GM1 mimic, with magnetic relaxation facilitating this discovery and SPR confirming the target−ligand interaction. In addition, using magnetic relaxation measurements and SPR we confirmed the interaction of galactose with CTB.

Galactose-carrying MRnS and dextran-carrying MRnS can detect CTB with a detection threshold of 40 pM and 16 nM, respectively. This level of sensitivity compares favorably with the detection limits of 727 nM for a fluorescent antibody approach,[36] 182 nM for a method that uses quantum dots coated with anti-CT antibodies,[37] and 54 nM for lactose-conjugated gold particles.[35] Toxin detection by magnetic relaxation and MRnS is also a rapid 5 min process that requires few reagents, consumes small amounts of sample, and utilizes a simple, single-step sample preparation protocol, involving easy-to-use and easy-to-read instrumentation. Also, the binding event can be easily recorded with a simple relaxometer without the need of complex NMR or MRI instrumentation.[38] These characteristics, combined with our reported results, highlight the potential value of MRnS and magnetic relaxation detection for the quick and selective assessment using molecular mimicry of carbohydrate−toxin interactions. Furthermore, our results indicate that the valency of the conjugated MRnS affects the $\Delta T2$ pattern. Consistent with previous reports on cell detection,[19] we found that the low-valency (LV) and high-valency (HV) galactose-carrying MRnS exhibited valency-dependent behaviors. The $\Delta T2$ response with LV MRnS followed an inversely proportional relationship with respect to toxin concentration, while the HV MRnS followed a directly proportional relationship with respect to toxin concentration. The inherently high valency dextran-carrying MRnS also exhibited a directly proportional relationship with the toxin levels, causing increases in $\Delta T2$.

MRnS can be a valuable tool to identify weak yet important molecular interactions. For instance, the interaction between CTB and glucose has not been previously reported. In the past, direct examination of the CTB−glucose binding by fluorescence analysis failed to detect any interaction between the two.[30] However, the three alternative assays used in this report (magnetic relaxation, SPR, and cell-based binding competition) all demonstrated an interaction between dextran and the CTB pentamer. It is interesting to note that dextran, a glucose polymer, is able to interact with CTB, whereas glucose has not been found to interact with the toxin in previous reports. A possible explanation for this difference could be the way the glucose molecule is presented for binding during the experimental setup. Perhaps, within the dextran polymer the units of glucose are displayed in such a way that they maximize interaction with CTB, facilitating binding. This interaction seems to be specific between dextran and CTB, as magnetic relaxation and SPR experiments carried out with the tetanus toxin (TTC) did not detect any interaction, even though the ganglioside receptors of TTC contain glucose. This is in line with previous reports that indicate that TTC interacts preferentially with GD1b and GT1b via the gangliosides' sialic acid residues.[31,32] Although the GM1−CTB crystal structure reveals a substantial contribution of the terminal galactose residue to toxin binding,[25,39] a role for other glycans in GM1−CTB interactions has also been suggested.[30]

Dextran-coated MRnS are substantially less expensive to prepare than galactose-carrying MRnS, which require the conjugation of the galactose molecule (galactopyranosyl nonanoic acid) on poly(acrylic acid)-coated nanoparticles. Additionally, the dextran-coated MRnS are less expensive than antibody-based detection technologies. Thus, MRnS−carbohydrate conjugates represent a sensitive, low-cost approach for the detection of CT and potentially other toxins. Particularly, dextran-coated iron oxide nanoparticles can be used for the quick CT detection and potential anticholera therapy. This is highly important in developing countries where the disease is rampant and efficient, urgently needing low-cost detection and treatment techniques. Although we have shown that dextran inhibits CT binding to the surface of a target cell, suggesting that dextran could potentially block productive intoxication of the target cell, further experiments are needed to establish the potential therapeutic value of dextran and dextran-coated MRnS.

In conclusion, our studies provide a proof-of-principle for the use of carbohydrate-carrying MRnS as molecular mimics for toxin detection. CT was the chosen target for this study, but the judicious screening of molecular libraries with MRnS should facilitate the identification of new toxin ligands for detection and treatment. Overall, this MRnS approach might be an alternative strategy for the development of sensitive diagnostic modalities and effective therapeutics, utilizing cell-surface receptors and small molecules, as opposed to antibodies.[40−44]

■ ASSOCIATED CONTENT

Supporting Information. Surface plasmon resonance analysis of tetanus toxin C fragment. This material is available free of charge via the Internet at http://pubs.acs.org.

■ AUTHOR INFORMATION

Corresponding Author

*Nanoscience Technology Center, University of Central Florida, 12424 Research Parkway, Suite 400, Orlando, FL 32826. Ph: 407-882-2843. Fax: 407-882-2819. E-mail: jmperez@mail.ucf.edu.

■ ACKNOWLEDGMENT

This study was supported by the NIH grant GM084331 awarded to J.M.P.

■ REFERENCES

(1) Alouf, J. E., and Popoff, M. R. (2006) *The comprehensive sourcebook of bacterial protein toxins*, 3rd ed., Academic Press, San Diego.

(2) Salyers, A. A., and Whitt, D. D. (2002) *Bacterial pathogenesis: a molecular approach*, 2nd ed., ASM Press, Washington, DC

(3) Kaittanis, C., Santra, S., and Perez, J. M. (2009) Emerging nanotechnology-based strategies for the identification of microbial pathogenesis. *Adv. Drug Delivery Rev. 62*, 408–23.

(4) Middlebrook, J. L., and Brown, J. E. (1995) Immunodiagnosis and immunotherapy of tetanus and botulinum neurotoxins. *Curr. Top. Microbiol. Immunol. 195*, 89–122.

(5) Sack, D. A., Sack, R. B., Nair, G. B., and Siddique, A. K. (2004) Cholera. *Lancet 363*, 223–33.

(6) Mabry, R., Brasky, K., Geiger, R., Carrion, R., Jr., Hubbard, G. B., Leppla, S., Patterson, J. L., Georgiou, G., and Iverson, B. L. (2006)

Detection of anthrax toxin in the serum of animals infected with Bacillus anthracis by using engineered immunoassays. *Clin. Vaccine Immunol. 13*, 671–7.

(7) Ezzell, J. W., Jr., and Abshire, T. G. (1992) Serum protease cleavage of Bacillus anthracis protective antigen. *J. Gen. Microbiol. 138*, 543–9.

(8) Panchal, R. G., Halverson, K. M., Ribot, W., Lane, D., Kenny, T., Abshire, T. G., Ezzell, J. W., Hoover, T. A., Powell, B., Little, S., Kasianowicz, J. J., and Bavari, S. (2005) Purified Bacillus anthracis lethal toxin complex formed in vitro and during infection exhibits functional and biological activity. *J. Biol. Chem. 280*, 10834–9.

(9) Rucker, V. C., Havenstrite, K. L., and Herr, A. E. (2005) Antibody microarrays for native toxin detection. *Anal. Biochem. 339*, 262–70.

(10) Homola, J., Dostalek, J., Chen, S., Rasooly, A., Jiang, S., and Yee, S. S. (2002) Spectral surface plasmon resonance biosensor for detection of staphylococcal enterotoxin B in milk. *Int. J. Food Microbiol. 75*, 61–9.

(11) Medina, M. B. (2006) Development of a fluorescent latex microparticle immunoassay for the detection of staphylococcal enterotoxin B (SEB). *J. Agric. Food Chem. 54*, 4937–42.

(12) Kawano, Y., Ito, Y., Yamakawa, Y., Yamashino, T., Horii, T., Hasegawa, T., and Ohta, M. (2000) Rapid isolation and identification of staphylococcal exoproteins by reverse phase capillary high performance liquid chromatography-electrospray ionization mass spectrometry. *FEMS Microbiol. Lett. 189*, 103–8.

(13) Carol, J., Gorseling, M. C., de Jong, C. F., Lingeman, H., Kientz, C. E., van Baar, B. L., and Irth, H. (2005) Determination of denaturated proteins and biotoxins by on-line size-exclusion chromatography-digestion-liquid chromatography-electrospray mass spectrometry. *Anal. Biochem. 346*, 150–7.

(14) Hakami, R. M., Ruthel, G., Stahl, A. M., and Bavari, S. (2010) Gaining ground: assays for therapeutics against botulinum neurotoxin. *Trends Microbiol. 18*, 164–72.

(15) Gaster, R. S., Hall, D. A., Nielsen, C. H., Osterfeld, S. J., Yu, H., Mach, K. E., Wilson, R. J., Murmann, B., Liao, J. C., Gambhir, S. S., and Wang, S. X. (2009) Matrix-insensitive protein assays push the limits of biosensors in medicine. *Nat. Med. 15*, 1327–32.

(16) Perez, J. M., Josephson, L., O'Loughlin, T., Hogemann, D., and Weissleder, R. (2002) Magnetic relaxation switches capable of sensing molecular interactions. *Nat. Biotechnol. 20*, 816–20.

(17) Perez, J. M., Simeone, F. J., Saeki, Y., Josephson, L., and Weissleder, R. (2003) Viral-induced self-assembly of magnetic nanoparticles allows the detection of viral particles in biological media. *J. Am. Chem. Soc. 125*, 10192–3.

(18) Kaittanis, C., Naser, S. A., and Perez, J. M. (2007) One-step, nanoparticle-mediated bacterial detection with magnetic relaxation. *Nano Lett. 7*, 380–3.

(19) Kaittanis, C., Santra, S., and Perez, J. M. (2009) Role of nanoparticle valency in the nondestructive magnetic-relaxation-mediated detection and magnetic isolation of cells in complex media. *J. Am. Chem. Soc. 131*, 12780–91.

(20) Nath, S., Kaittanis, C., Ramachandran, V., Dalal, N. S., and Perez, J. M. (2009) Synthesis, magnetic characterization, and sensing applications of novel dextran-coated iron oxide nanorods. *Chem. Mater. 21*, 1761–1767.

(21) Perez, J. M., Grimm, J., Josephson, L., and Weissleder, R. (2008) Integrated nanosensors to determine levels and functional activity of human telomerase. *Neoplasia 10*, 1066–72.

(22) Grimm, J., Perez, J. M., Josephson, L., and Weissleder, R. (2004) Novel nanosensors for rapid analysis of telomerase activity. *Cancer Res. 64*, 639–43.

(23) Spangler, B. D. (1992) Structure and function of cholera toxin and the related Escherichia coli heat-labile enterotoxin. *Microbiol. Rev. 56*, 622–47.

(24) Viswanathan, V. K., Hodges, K., and Hecht, G. (2009) Enteric infection meets intestinal function: how bacterial pathogens cause diarrhoea. *Nat. Rev. Microbiol. 7*, 110–9.

(25) Merritt, E. A., Sarfaty, S., van den Akker, F., L'Hoir, C., Martial, J. A., and Hol, W. G. (1994) Crystal structure of cholera toxin B-pentamer bound to receptor GM1 pentasaccharide. *Protein Sci. 3*, 166–75.

(26) Santra, S., Kaittanis, C., Grimm, J., and Perez, J. M. (2009) Drug/dye-loaded, multifunctional iron oxide nanoparticles for combined targeted cancer therapy and dual optical/magnetic resonance imaging. *Small 5*, 1862–8.

(27) Koch, A. M., Reynolds, F., Kircher, M. F., Merkle, H. P., Weissleder, R., and Josephson, L. (2003) Uptake and metabolism of a dual fluorochrome Tat-nanoparticle in HeLa cells. *Bioconjugate Chem. 14*, 1115–21.

(28) Shen, T., Weissleder, R., Papisov, M., Bogdanov, A., Jr., and Brady, T. J. (1993) Monocrystalline iron oxide nanocompounds (MION): physicochemical properties. *Magn. Reson. Med. 29*, 599–604.

(29) Massey, S., Banerjee, T., Pande, A. H., Taylor, M., Tatulian, S. A., and Teter, K. (2009) Stabilization of the tertiary structure of the cholera toxin A1 subunit inhibits toxin dislocation and cellular intoxication. *J. Mol. Biol. 393*, 1083–96.

(30) Mertz, J. A., McCann, J. A., and Picking, W. D. (1996) Fluorescence analysis of galactose, lactose, and fucose interaction with the cholera toxin B subunit. *Biochem. Biophys. Res. Commun. 226*, 140–4.

(31) Angstrom, J., Teneberg, S., and Karlsson, K. A. (1994) Delineation and comparison of ganglioside-binding epitopes for the toxins of Vibrio cholerae, Escherichia coli, and Clostridium tetani: evidence for overlapping epitopes. *Proc. Natl. Acad. Sci. U.S.A. 91*, 11859–63.

(32) Holmgren, J., Elwing, H., Fredman, P., and Svennerholm, L. (1980) Polystyrene-adsorbed gangliosides for investigation of the structure of the tetanus-toxin receptor. *Eur. J. Biochem. 106*, 371–9.

(33) Arnon, S. S., Schechter, R., Inglesby, T. V., Henderson, D. A., Bartlett, J. G., Ascher, M. S., Eitzen, E., Fine, A. D., Hauer, J., Layton, M., Lillibridge, S., Osterholm, M. T., O'Toole, T., Parker, G., Perl, T. M., Russell, P. K., Swerdlow, D. L., and Tonat, K. (2001) Botulinum toxin as a biological weapon: medical and public health management. *JAMA 285*, 1059–70.

(34) Kaittanis, C., Nath, S., and Perez, J. M. (2008) Rapid nanoparticle-mediated monitoring of bacterial metabolic activity and assessment of antimicrobial susceptibility in blood with magnetic relaxation. *PLoS One 3*, e3253.

(35) Schofield, C. L., Field, R. A., and Russell, D. A. (2007) Glyconanoparticles for the colorimetric detection of cholera toxin. *Anal. Chem. 79*, 1356–61.

(36) Rowe-Taitt, C. A., Cras, J. J., Patterson, C. H., Golden, J. P., and Ligler, F. S. (2000) A ganglioside-based assay for cholera toxin using an array biosensor. *Anal. Biochem. 281*, 123–33.

(37) Goldman, E. R., Clapp, A. R., Anderson, G. P., Uyeda, H. T., Mauro, J. M., Medintz, I. L., and Mattoussi, H. (2004) Multiplexed toxin analysis using four colors of quantum dot fluororeagents. *Anal. Chem. 76*, 684–8.

(38) Lee, H., Sun, E., Ham, D., and Weissleder, R. (2008) Chip-NMR biosensor for detection and molecular analysis of cells. *Nat. Med. 14*, 869–74.

(39) Merritt, E. A., Sixma, T. K., Kalk, K. H., van Zanten, B. A., and Hol, W. G. (1994) Galactose-binding site in Escherichia coli heat-labile enterotoxin (LT) and cholera toxin (CT). *Mol. Microbiol. 13*, 745–53.

(40) Chang, P. V., Chen, X., Smyrniotis, C., Xenakis, A., Hu, T., Bertozzi, C. R., and Wu, P. (2009) Metabolic labeling of sialic acids in living animals with alkynyl sugars. *Angew. Chem., Int. Ed. Engl. 48*, 4030–3.

(41) Hangauer, M. J., and Bertozzi, C. R. (2008) A FRET-based fluorogenic phosphine for live-cell imaging with the Staudinger ligation. *Angew. Chem., Int. Ed. Engl. 47*, 2394–7.

(42) Laughlin, S. T., Baskin, J. M., Amacher, S. L., and Bertozzi, C. R. (2008) In vivo imaging of membrane-associated glycans in developing zebrafish. *Science 320*, 664–7.

(43) Laughlin, S. T., and Bertozzi, C. R. (2009) Imaging the glycome. *Proc. Natl. Acad. Sci. U.S.A. 106*, 12–7.

(44) Singh, A. K., Harrison, S. H., and Schoeniger, J. S. (2000) Gangliosides as receptors for biological toxins: development of sensitive fluoroimmunoassays using ganglioside-bearing liposomes. *Anal. Chem. 72*, 6019–24.